

A Variable-Structure Robot Hand That Uses the Environment to Achieve General Purpose Grasps

Yoav Golan , Amir Shapiro , and Elon D. Rimon 

Abstract—Modern robotic grippers are either specialized and simple, complex and general purpose, or soft and compliant hands. The first provide high reliability but are limited in the range of objects they grasp. Compliant or soft grippers can grasp wide ranges of objects, but are not yet reliable enough for real-world applications. This letter presents a novel variable-structure general purpose robotic hand. The planar-acting hand has a minimalistic structure that can adapt itself against the environment to fit a wide range of objects. The single motor, multi-finger hand utilizes a novel principle of re-arranging its structure prior to grasping. This is achieved by pressing the hand against the environment and performing a series of adjustment moves, to best suit the hand for the object to be grasped. The design and method of operation of the hand is explained. Then, a technique for determining the set of adjustments needed to re-arrange the hand according to the desired grasp is sketched. Real-world experiments are performed with the hand, showing its ability to re-arrange itself and grasp previously unseen objects. Source code for the simulations and experiments is supplemented to the paper, as well as a video clip of the variable-structure hand in action.

Index Terms—Grippers and other end-effectors, manipulation planning, grasping, mechanism design.

I. INTRODUCTION

AS ROBOTIC grasping and manipulation applications are rapidly expanding, the need for reliable grasping of objects is ever growing. Despite many contributions of grasping research over the years, industrial grippers are still quite simple. Typical industrial grippers include parallel-jaw grippers, vacuum grippers, or specialized grippers designed to grasp specific objects. What these grippers have in common is their ease of operation and high reliability. Each of these grippers has a single degree of freedom. I.e., the gripper is either activated and gripping, or it is deactivated and not gripping the object. This simplicity allows

Manuscript received February 24, 2020; accepted June 5, 2020. Date of publication June 19, 2020; date of current version June 30, 2020. This letter was recommended for publication by Associate Editor Zhenhua Xiong and Editor Hong Liu upon evaluation of the reviewers' comments. This work was supported in part by ISF under Grant 1253/14 and in part by the Helmsley Charitable Trust through the Agricultural, Biological and Cognitive Robotics Center of Ben-Gurion University. (Corresponding author: Yoav Golan.)

Yoav Golan and Amir Shapiro are with the Department of Mechanical Engineering, Ben-Gurion University, Beer Sheva 8410501, Israel (e-mail: yoavgo@post.bgu.ac.il; ashapiro@bgu.ac.il).

Elon D. Rimon is with the Department of Mechanical Engineering, Technion - Israel Institute of Technology, Haifa 3200003, Israel (e-mail: rimon@technion.ac.il).

This article has supplementary downloadable material available at <http://ieeexplore.ieee.org>, provided by the authors.

Digital Object Identifier 10.1109/LRA.2020.3003885

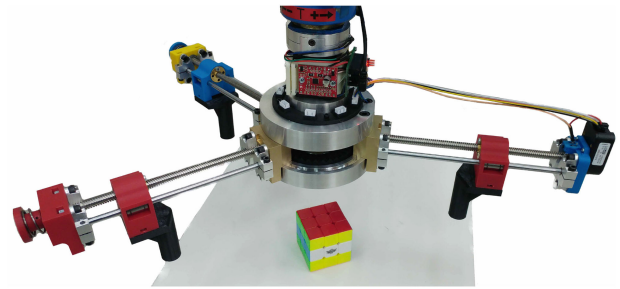


Fig. 1. The variable-structure hand, shown here with three digits. Each of the downward pointing digit fingertips can be extended, retracted, or have its relative angle changed.

industrial grippers to be easily controlled in a predictable and reliable manner [1].

The price of simplicity and reliability, however, is lack of flexibility. A parallel-jaw gripper designed to grasp a 3/8" pipe will *not* be very good at grasping small boxes. A specialized hand designed to grasp the front-right door of a car will fail to grasp a rear-right door. Modern robot hand research focuses on the generalization of industrial grippers. Some researchers have focused on “classic” grippers and sophisticated means of decision making to securely grasp items. For instance, Mahler *et al.* [2] use a vacuum gripper or parallel-jaw gripper to perform bin picking tasks. Machine learning is used to generalize object grasps from a training set, allowing the system to select the correct gripper, item, and approach to perform a picking operation. Other researchers have elected to develop underactuated hands that can adapt to objects, such as Backus [3] and Dollar [4]. The emerging field of soft robotics [5] has produced many interesting grippers designed to grip a variety of objects, e.g. [6]–[9]. While underactuated and soft hands are making significant progress towards industrial use, they still cannot compare with the reliability, strength and robustness of classic industrial grippers.

This paper describes a minimalistic, planar-acting robot hand that uses the *environment* to change its structure. The hand uses a single degree of freedom (DOF), driven by a single actuator. The hand is not soft, underactuated or shape conforming. Rather, it is rigid and predictable in its operation, similar to classical industrial grippers. Adaptability is achieved by adjusting the hand's structure before grasping. In other words, the hand is tailored to the object it is meant to grasp, before attempting to grasp the object. In contrast to specialized hands designed to grasp specific objects, there is no need to redesign and manufacture

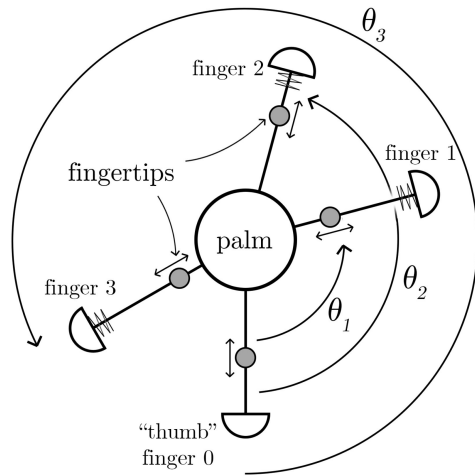


Fig. 2. A schematic top view of a k -finger configurable hand. The “thumb” maintains its angle of 0° . The other fingers each have a variable angle θ_i relative to the thumb. Except for the thumb, the fingers have plungers at their distal ends. All the digits, including the thumb, have downward pointing fingertips that can extend or retract towards the hand’s center.

a new hand whenever a new object is encountered. Instead, our *variable-structure hand* can be adjusted using the environment prior to its use.

The variable-structure hand works as follows. The robot arm observes an object and determines the desired grasp, without being constrained by the hand structure. The robot arm then performs a series of adjustments to the hand configuration, to suit it to the best grasp of the given object. Our variable-structure hand is the exact opposite of approaches like Mahler’s [2], that dedicate their effort to selecting the best possible grasp of an object using available *fixed structure* grippers. The main caveat of our approach is the time needed to perform the physical alteration of the hand prior to grasping. However, this extra time is only needed when grasping new types of objects, and is not necessary when grasping similar items sequentially. Therefore, we expect that a variable-structure hand will save time and costs in robotic tasks where a gripper must grasp multiple items of one type, and later grasp multiple items of another type. Furthermore, when different items are to be grasped with enough time between them to re-arrange the hand (a time that will eventually become seconds), our system will allow generalized grasping without wasting system operation time.

The paper makes the following contributions. The first is a novel idea showing how the environment can be used to augment a single degree-of-freedom hand, effectively endowing the hand with two degrees of freedom for each finger (see Fig. 2). This means that the hand has full-freedom of grasping arbitrary 2-D objects using only a single motor. The second contribution is a practical design of such a working hand, demonstrated in real-world experiments. The third contribution is a novel grasp selection algorithm that utilizes the hand’s variable-structure property. The algorithm selects the best grasp for a given object, taking into consideration the geometric constraints imposed by the hand. The fourth contribution, which is only sketched in this paper, is a novel technique for synthesizing the adjustments that

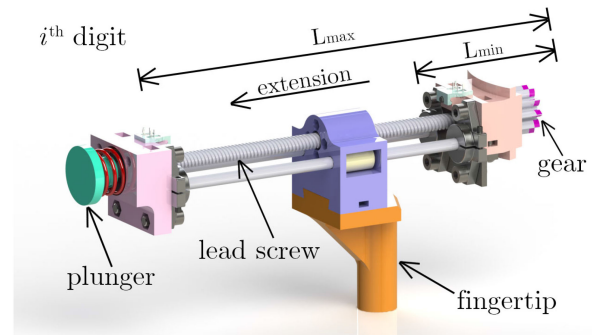


Fig. 3. A CAD rendering of the finger module. The fingertip (orange) is a simple cylinder driven by a lead screw. The lead screw is powered by a spur gear (gray and violet) powered by two opposing face gears not seen in this figure. A spring-loaded plunger (green) pushes the spur gear along its axis, which allows decoupling from the face gears.

use the environment to reconfigure the hand to a chosen grasp. The hand’s adjustment synthesis is available in [10].

The paper is structured as follows. Section II explains the hand mechanism basic design that allows adjustment of its structure using the environment. Section III details the algorithm used to observe an object and determine the desired grasp. Section IV sketches the method of synthesizing and executing the series of environment interactions needed to adjust the hand structure according to the desired grasp. Section V presents experiments demonstrating our robotic hand performing adjustments against the environment and grasping a variety of objects. Section VI summarizes the results and describes future work.

II. DESIGN AND METHOD OF OPERATION

This section explains how the design of our robotic hand allows a change in the hand structure. Specifically, how the *relative angle* between the digits and the *distance* of the fingertips from the hand center can be changed freely using the environment.

A. Hand Design Overview

The robotic hand consists of a single motor, a central body (the *palm*), and a number of digits. A CAD rendering of a finger module can be seen in Fig. 3. The fingertip (orange) is driven by a lead-screw powered by a spur gear. One distinguished digit, the *thumb*, has a few small design changes that will be detailed later. The user can determine how many digits the hand should be equipped with. Adding or removing a digit requires partial disassembly of the hand. Therefore, changing the number of fingers is typically a pre-determined choice, and not part of normal operation. A schematic hand with four digits can be seen in Fig. 2, a photograph of a three fingered hand can be seen in Fig. 1. Most classic single actuator grippers use two to four digits. Therefore, most of our figures and demonstrations use these quantities. Each digit has a downward pointing *fingertip* that can move along its length. In our examples the fingertips are simple cylinders that can be set at an offset to grasp smaller or larger object sets. The cylindrical fingertips can easily be replaced by more complex members, such as compliant [11] or

variable-friction fingertips [12]. The fingertips are the members that come in contact and securely grasp an object.

In general, fewer fingers incur shorter adjustment times, and more freedom in finger placement (there are fewer fingers to interfere). A higher number of fingers generally leads to higher quality grasps, since there are more contact points. Theoretically, three frictionless fingertips are sufficient to grasp any planar, polygonal object—except for objects with parallel edges [13]. As it happens, rectangular objects are extremely common, and four digits are needed to grasp them under low-friction conditions. Selecting the optimal number of fingers is not the concern of this paper. Therefore, we choose the number of fingers based on the operator’s intuition.

The hand’s central body, or *palm*, acts as a hub, connecting the digits and the motor. Two opposing face gears centered in the palm are powered by the single motor. Each digit interacts with the motor-activated gear system. When the motor is powered, all fingertips *retract or extend simultaneously* at the same rate. The direction of retraction is towards the center of the hand, and vice-versa with extension.

Each finger is mounted on a circular rail, and can be placed at different angles on the palm. The thumb is the only digit that is fixed to the palm at an angle $\theta_0 = 0^\circ$ relative to the hand. Another finger can be fixed at a variable angle relative to the thumb, say at $\theta_1 = 120^\circ$, and so on. It should be noted that digits cannot be placed too close to each other due to physical constraints. Each digit occupies a “wedge” of δ degrees. In our design, $\delta = 45^\circ$. Thus, at most $\lfloor 360^\circ/\delta \rfloor$ digits can be added to the hand.

As previously mentioned, the thumb is the only digit fixed to the palm. The fingers are not fixed to the palm, and therefore can potentially rotate about its center, changing their angles. This motion is prohibited by the gearing of the hand. The face gears, powered by the motor, are typically meshed with each digit’s driving gear. This *gear locking* prevents any change of the finger’s orientation. In regular operation the fingers are immobile, and the fingertips can be retracted or extended together using the hand’s motor. Next we will explore how the hand’s structure can be altered.

B. Altering the Hand’s Structure

Let us first define the hand’s structure. We examine a hand where a user has installed $k \geq 2$ digits. Each of the digits has an angle relative to the thumb: θ_i , $i = 0 \dots k - 1$. Each of the k finger mechanisms has a downward pointing fingertip, located at a distance d_i from the center of the hand. Therefore, the structure of the hand is described as a vector: $\vec{C} = (\vec{\theta}, \vec{d}) = (\theta_0 = 0^\circ, \theta_1, \dots, \theta_{k-1}, d_0, d_1, \dots, d_{k-1})$. We can alter the hand’s structure by changing the finger orientations $\vec{\theta}$, and/or changing the fingertip distances \vec{d} . Let us examine each of these options separately.

1) *Changing Finger Orientation*: We have already established that a finger cannot normally be rotated about the palm due to gear locking. Each finger has a spring loaded *plunger* at its distal end, furthest from the palm (see Fig. 3). When the plunger is pressed, it compresses the spring, and displaces the internal drive mechanism of the finger. The drive mechanism of the finger

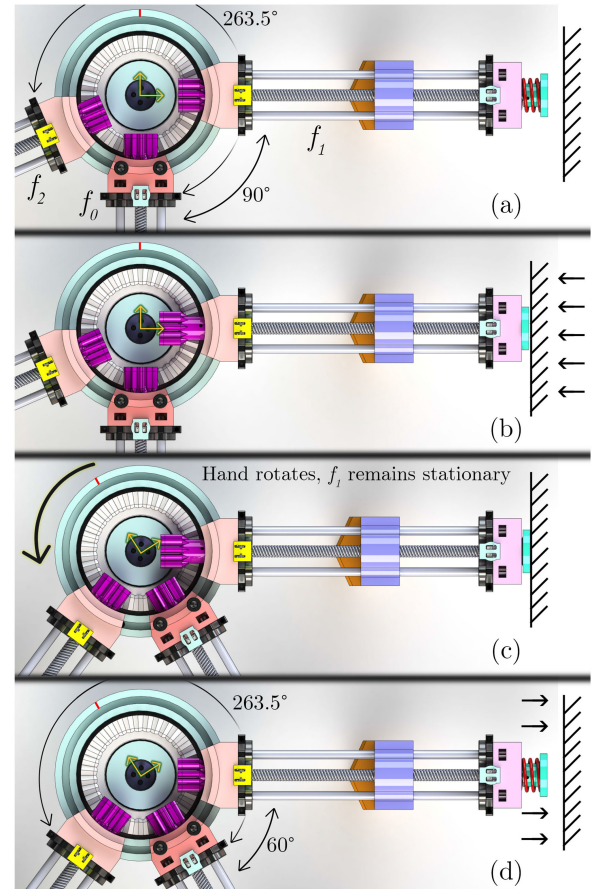


Fig. 4. The adjustment of a finger’s orientation, viewed with the top portion of the hand removed. (a) The initial state of a three fingered hand. (b) The plunger of the rightmost finger is pressed, disconnecting the finger’s gear from the larger face gear. (c) Rotation of the hand. A motor in the robotic arm rotates the hand’s base, face gear, and fingers f_0 and f_2 . The rightmost finger f_1 remains stationary. The hand frame centered at the palm rotates with the hand and is stationary relative to the thumb f_0 . (d) The plunger of f_1 is released, re-engaging the gears. The relative angle of f_1 is now altered to $\theta_1 = 60^\circ$, while $\theta_2 = 263.5^\circ$ remains unchanged.

includes a spur gear that meshes with the face gears of the palm. When the plunger is pressed, the spur gear moves and *decouples* from the face gear. At this instant, the gear lock that prevented the finger’s rotation is no longer in effect. Therefore, the finger can now be rotated about the palm. This action is shown in Fig. 4. To rotate a finger, one must press the finger’s plunger, then rotate the finger to the desired angle. In practice, the entire fixed-shape hand is rotated while the single finger remains static, resulting in a relative rotation of the finger. The hand is rotated by the last joint of the robotic arm. Once at the desired angle, the plunger is released, and the spring returns the gear mechanism to its default state, thus locking the finger at its new state.

This is where the robot arm and the environment are useful in changing the hand’s structure. The robot arm moves the hand towards a rigid, static body. This can be a wall in the workspace, or even part of the robot arm. The hand is pressed— finger plunger first— against the wall, rotated, and released. As an example, assume a hand structure at $(\theta_0^0, \theta_1^0, \theta_2^0, d_0^0, d_1^0, d_2^0) = (0^\circ, 90^\circ, 293.5^\circ, 100 \text{ mm}, 100 \text{ mm}, 100 \text{ mm})$, as is the case in

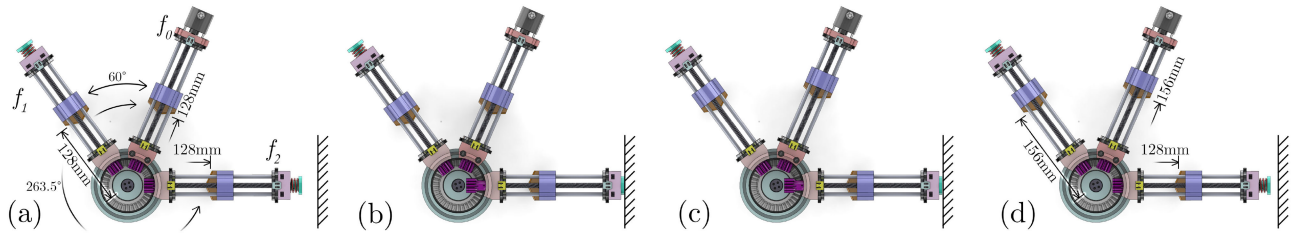


Fig. 5. The redistancing of a fingertip. After the restructuring in Fig. 4, the hand structure is at $(0^\circ, 60^\circ, 293.5^\circ, 100 \text{ mm}, 100 \text{ mm}, 100 \text{ mm})$. In (a) the hand motor has already been rotated twice, resulting in a structure $(0^\circ, 60^\circ, 293.5^\circ, 128 \text{ mm}, 128 \text{ mm}, 128 \text{ mm})$. (b) The plunger of f_2 is pressed against the wall, decoupling its gear from the hand motor. (c) The hand motor is rotated twice again, extending the fingertips of f_0 and f_1 , but not the decoupled f_2 . (d) f_2 's plunger is unpressed, and the gear recouples. The hand structure is now $\vec{C}_3 = (0^\circ, 60^\circ, 293.5^\circ, 156 \text{ mm}, 156 \text{ mm}, 128 \text{ mm})$. All distances are from the fingertip centers to the palm's center.

Fig. 4(a). If we want to rotate a finger, we first press the finger's plunger against the environment (Fig. 4(b)). Next, we rotate the entire hand. Each of the digits, except for the now-decoupled finger, rotates. Say we rotate the hand 30° counterclockwise (Fig. 4(c)). Finally, we release the finger's plunger (Fig. 4(d)). The new structure is now $(0^\circ, 60^\circ, 293.5^\circ, 100 \text{ mm}, 100 \text{ mm}, 100 \text{ mm})$. Thus we have altered the relative orientation of the fingers.

2) *Changing Fingertip Distances*: Changing the fingertip distances can be achieved in two ways. First, by rotating the motor, all of the fingertips are extended or retracted equally. Let us say that the hand structure is at $(0^\circ, 60^\circ, 293.5^\circ, 100 \text{ mm}, 100 \text{ mm}, 100 \text{ mm})$. If we rotate the motor two revolutions, the gear ratio results in a global change of 28 mm, so that $\vec{C}_2 = (0^\circ, 60^\circ, 293.5^\circ, 128 \text{ mm}, 128 \text{ mm}, 128 \text{ mm})$. This change of distances is always *equal* for all digits. Therefore, the relative distance between the fingertips remains constant.

The second way of changing fingertip distances allows true flexibility. In this method, first one of the finger's plungers is pressed against the environment, similarly to the angular change. While a plunger is pressed, the finger's gear is decoupled. Therefore, if the motor rotates, the fingertip will not move, while the other fingertips move with an equal distance change. This creates a *relative distance change*. As an example, let us continue at structure \vec{C}_2 , shown in Fig. 5(a). We press the plunger on the third digit (Fig. 5(b)), then rotate the motor two additional revolutions (Fig. 5(c)). Again, the fingertips will extend 28 mm except for the third fingertip, thus resulting in a new hand structure at $\vec{C}_3 = (0^\circ, 60^\circ, 293.5^\circ, 156 \text{ mm}, 156 \text{ mm}, 128 \text{ mm})$, shown in Fig. 5(d).

Two important points should be noted. a) The thumb does not have a plunger and cannot be decoupled. This is not a crucial design factor, and does not impact the hand's reconfiguration ability. b) The fingertips *cannot* be independently extended or retracted. Therefore, attaining a desired distance configuration is a non-trivial problem, addressed later.

III. SELECTING THE BEST GRASP

This section describes a novel approach for selecting a grasp configuration for an object. When using a *non-configurable* robot hand, any grasp configuration must conform to the hand

shape. For instance, if an equidistant, three-fingered hand (e.g. [14]) is used, only grasp configurations that constitute equilateral triangles may be considered. Our approach utilizes the reconfiguration ability of the hand to maximize grasp quality by relaxing the finger positioning constraints. A *grasp configuration* is defined as the fingertip placements on the object's perimeter. A *hand structure* is defined as a combination of the grasp configuration and the location of the hand's center. Although our hand allows total freedom in grasp configuration selection, physical constraints still exist, so not every hand structure is possible.

Let us first examine the decision process for finger placement—the grasp configuration. The object is given as a polygon in configuration space. I.e, the object has been represented as a polygon, and dilated by the radius of the fingertips. This means that any point on the boundary of the configuration-space object corresponds to a fingertip-object contact point. The friction coefficient between the fingertips and the object μ is known, as is the number of fingers k . We now proceed to choose the grasp configuration. To do this, we use Monte-Carlo simulation of grasp configurations. The polygon perimeter is discretized as a set of points, each with its own location and normal direction. We then randomly place k fingertips at different points on the polygon perimeter, and test the grasp quality. There are many grasp quality measures, and it is not this paper's intention to advocate one or the other. Our procedure grants the user the option to choose between *wrench space sphere radius* and *grasp matrix ellipsoid* quality measures, although any other quality measure can be used. These quality measures and others can be found in [15, pp. 321-348].

The grasp is evaluated, and its quality is marked according to the guidelines of the quality measure. If the grasp is found to be immobilizing, the grasp configuration enters a list of possible grasp configurations. After exhausting the user-defined number of grasp attempts, the list is sorted by grasp quality. We now have a list of immobilizing grasp configurations, sorted by their quality. While all of these grasps are immobilizing, the physical structure of the hand imposes another constraint; not all of these immobilizing grasp configurations are actually feasible. A candidate hand structure is *feasible* if a hand center exists for the given the grasp configuration. Therefore, we can examine each grasp configuration to determine its potential as a feasible hand structure. Starting from the best grasp configuration in the list,

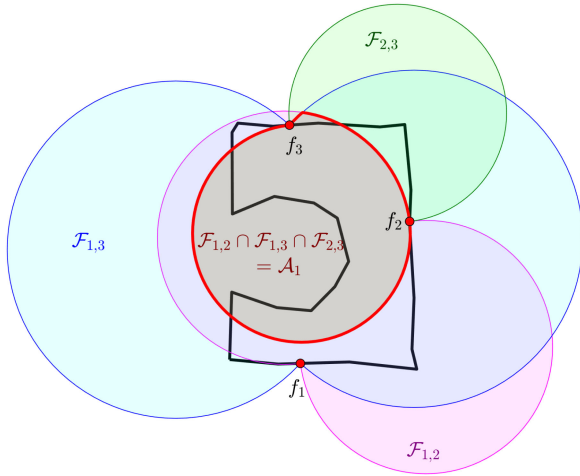


Fig. 6. An example of the angular geometric constraints of finger placement. The object (black outline) is grasped by three fingertips (red dots). The angle between two digits must be at least $\delta = 45^\circ$. For each pair of fingers, the union of two discs bounds the hand's center area. In this instance, fingers 1 and 2 only allow the placement of the hand center within the double-circle magenta shape $F_{1,2}$. The intersection of all the pairs results in the allowed area (red border).

we test to see if a hand structure can be synthesized. I.e, we test to see if a hand center point P exists with its fingers at the candidate grasp configuration. This test is performed by converting the physical hand limitations to three geometric constraints.

Consider the point P representing the center of the hand. The first physical limitation of P is angular. Two neighboring digits cannot be at angles less than δ apart. This limitation can be described geometrically as two overlapping discs, shown in Fig. 6. Consider two fingertip placements, f_i and f_j . The hand center P must be located such that the digit vectors are no more than δ degrees apart, or:

$$\angle(\overrightarrow{f_i - \bar{P}}, \overrightarrow{f_j - \bar{P}}) \geq \delta. \quad (1)$$

The set of points P that conform to this rule lie within the union of two overlapping discs. Each disc is bounded by f_i and f_j . Each point on the perimeter of either disc is such that $\angle(\overrightarrow{f_i - \bar{P}}, \overrightarrow{f_j - \bar{P}}) = \delta$. If the distance between f_i and f_j is $d_{i,j}$, then the radii of the two discs are:

$$r_{i,j} = \frac{d_{i,j}}{2 \sin(\delta)}. \quad (2)$$

The center of the hand, therefore, must lie within the area:

$$\mathcal{F}_{i,j} = \mathcal{F}_{i,j}^1 \cup \mathcal{F}_{i,j}^2 \quad (3)$$

where $\mathcal{F}_{i,j}^1$ and $\mathcal{F}_{i,j}^2$ are the two discs with radius $r_{i,j}$ that have f_i and f_j lying on their perimeters. The hand center must lie in this area for every pair of fingers f_i, f_j . Therefore, the hand's center must lie within the area \mathcal{A}_1 :

$$\mathcal{A}_1 = \bigcap \mathcal{F}_{i,j} \text{ for } 1 \leq i, j \leq k, i \neq j. \quad (4)$$

This constraint can be seen in Fig. 6 for a three-finger hand.

The second constraint is that the hand center P must lie within a circle of radius L_{max} centered at each fingertip placement, where L_{max} is the maximal extension of a fingertip. Therefore,

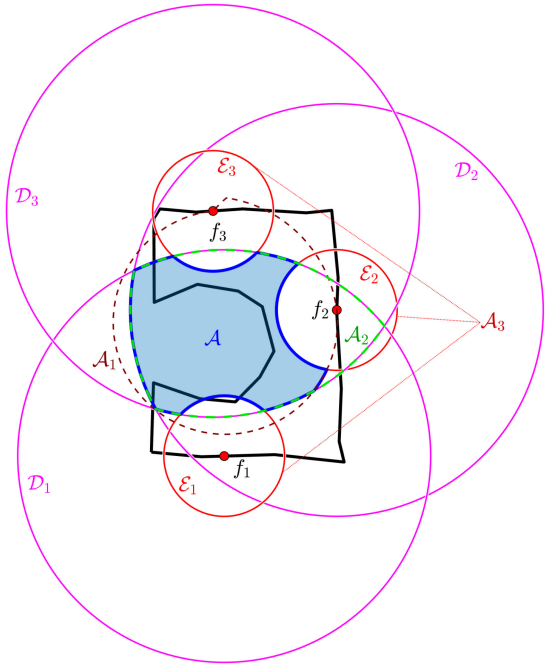


Fig. 7. An continuation of the example from Fig. 6. The object is grasped by three fingertips (red dots). The hand center must lie within a distance of L_{max} from each fingertip (magenta circles). The intersection of these circles is \mathcal{A}_2 (dashed green curves). The hand center cannot lie within L_{min} from any fingertip (red circles). The union of these circles is \mathcal{A}_3 . To conform with angle restrictions, the hand center must lie inside the area \mathcal{A}_1 (brown dashed curves). The blue area, marked \mathcal{A} , is the result of these restrictions, where the hand center can be placed.

the hand center must lie within the area \mathcal{A}_2 :

$$\mathcal{A}_2 = \bigcap_{i=1}^k \mathcal{D}_i \quad (5)$$

where \mathcal{D}_i is a circle of radius L_{max} centered at the i^{th} fingertip placement. This can be seen in Fig. 7, as magenta circles surrounding the fingertip placements.

Similarly, the hand center cannot lie too close to a fingertip placement, since there is a minimum extension L_{min} . Therefore, the hand center *cannot* lie within the area \mathcal{A}_3 :

$$\mathcal{A}_3 = \bigcup_{i=1}^k \mathcal{E}_i \quad (6)$$

where \mathcal{E}_i is a circle of radius L_{min} centered at the i^{th} fingertip placement. This can be seen in Fig. 7, as red circles surrounding the fingertip placements.

Finally, we combine the geometric constraints to obtain the valid area for the hand center. Any point P in this area is a physically feasible placement for the hand center:

$$\mathcal{A} = \mathcal{A}_1 \cap \mathcal{A}_2 \cap \bar{\mathcal{A}}_3, \quad (7)$$

where $\bar{\mathcal{A}}_3 = \mathbb{R}^2 - \mathcal{A}_3$. This area is illustrated in Fig. 7.

Any point in \mathcal{A} that allows a squeezing grasp of the object is valid, and as far as grasp quality they are identical. However, some hand center positions are better in other regards. We can identify *special centers* that have certain advantages. For

instance, a special center for three-fingered hands is the center of the circle defined by the three fingertip placements. This center has two advantages: 1) Each of the three fingertips is equidistant from the center. If the previous grasp configuration was also equidistant, the hand's distances adjustment procedure is *exceedingly short*. 2) If we define a triangle by the three fingertip placements, we note that extending or retracting the fingertips maintains a similar triangle. Similar triangle formations can be used to compute *caging regions* on polygons [16], potentially increasing grasp reliability and robustness using *caging grasps* [17].

If the preferred hand center is not feasible, one prefers hand centers that require shorter adjustment procedures of the hand. Each hand center P_i corresponds with a hand structure $C_i = (\vec{\theta}_i, \vec{d}_i)$. Starting from the hand's current structure, C_0 , each of the alternative structures, C_i , may take a different number of adjustments to achieve. Therefore, we construct adjustment procedures for every structure, as mentioned in the following Section IV. After synthesizing the adjustment procedure for each candidate hand structure, we choose the hand center that requires the shortest adjustment procedure. At this point, a number of valid hand structures have been found. In the next section, we detail the method of constructing and executing the adjustment procedure, which allows us to select and utilize one of these hand structures.

IV. SYNTHESIS OF THE HAND ADJUSTMENT PROCEDURE

The hand's *adjustment procedure* is a series of adjustments that transforms a hand from a start structure C_S to a target structure C_T . There are two main parts of an adjustment procedure—a change of digit angles, and a change of fingertip distances. Each of these parts is solved separately, and the solutions are combined into a final procedure. For lack of space, the algorithmic aspects of the adjustment procedure are described in a technical report [10]. Here we present the main principles of the hand adjustment procedure and provide illustrative examples. A three-finger version of the full adjustment procedure can be examined in the supplementary Matlab code joined with this paper [18].

Adjusting the digit angles is fairly straightforward, as each finger needs to be adjusted only once. There is always at least one finger whose angle can be adjusted to its target angle. This concept is proven in [10]. As an example for the angle adjustment procedure, consider the case where $C_S = (0, 45^\circ, 90^\circ, 90 \text{ mm}, 80 \text{ mm}, 100 \text{ mm})$, and $C_T = (0, 127.98^\circ, 206.77^\circ, 120.8 \text{ mm}, 198.3 \text{ mm}, 79.7 \text{ mm})$. The minimal extension for all three digits is $L_{min} = 70 \text{ mm}$. The maximal extension for digit 0 (the thumb) is $L_{max} = 213.7 \text{ mm}$, and the maximal extension for digits 1 and 2 is $L_{max} = 201 \text{ mm}$. First, we examine the angle adjustment problem. Digit 1 cannot be rotated from its current angle, $\theta_{S,1} = 45^\circ$, to its target $\theta_{T,1} = 127.98^\circ$, because digit 2 is in the way. Since there is always at least one digit that can be rotated to its target, it follows that digit 2 can be rotated. After rotating digit 2 to its target angle $\theta_{T,2} = 206.77^\circ$, we can rotate digit 1, thus completing the angular adjustment in $k - 1$ steps.

Next consider the change of *fingertip distances*, measured from the hand's center. Given a starting digit-length configuration, $\vec{d}_S = (d_{S,0}, d_{S,1}, \dots, d_{S,k-1})$, a series of digit length changes is required to achieve a target $\vec{d}_T = (d_{T,0}, d_{T,1}, \dots, d_{T,k-1})$. We can either change the distances of all fingertips, or change the distances of all fingertips except one, which is released by pressing its plunger against the environment. The extension of any digit may not exceed the minimal and maximal allowed extensions. We solve the extension/retraction planning problem using an analytic approach that is time-efficient even for multiple fingers [10]. The output of our algorithm is a series of distance changes needed to achieve the target fingertip distances. For instance, let the start and target distances be $\vec{d}_S = (90, 80, 100)$ and $\vec{d}_T = (120.8, 198.4, 79.7)$. The output will be the following: 1) "Press Finger 2, change the distances of fingertips 0 and 1 by 51.1 mm". The fingertip distances are now $\vec{d}_1 = (141.1, 131.1, 100)$. 2) "Change all distances by 67.2 mm". The fingertip distances are now $\vec{d}_2 = (208.3, 198.3, 167.2)$. 3) "Press Finger 1, change the distances of fingertips 0 and 2 by -87.5 mm ". The fingertip distances are now $\vec{d}_3 = (120.8, 198.3, 79.7)$ —the target distances. Note that at no point did the distances exceed the extension/retraction limits.

Combining the digits' angle and distance adjustments is fairly straightforward. We prioritize the distance adjustments over the angular adjustments, and perform an angular adjustment along with a distance adjustment when permitted. In our example, the first instruction would be 1) "Press Finger 2, change the distances of fingertips 0 and 1 by 51.1 mm while rotating the hand by 116.77° ". The next instruction is 2) "Change all distances by 67.2 mm". The final instruction is 3) "Press Finger 1, change the distance of fingertips 0 and 2 by -87.5 mm while rotating the hand by 82.98° ". This brings us to the distal and angular target structure of the hand. In this case, the angle adjustments aligned nicely with the extension adjustments. If they do not, we perform the remaining angular adjustments after the extension adjustments have been resolved. There are at most $k - 1$ angle changes. The number of extension adjustments depends on several factors. The upper bound is log-linear in k , and logarithmic in the distance of the start/target from the fingertip limits [10].

V. EXPERIMENTS

This section describes experiments performed with a three-finger hand. The experimental setup, both real and simulated, is depicted in Fig. 9. In our experiments we used a Motoman UP6 6-DOF robotic arm connected to the hand.

In order to demonstrate the capabilities of the variable-structure hand, we performed a number of full and partial grasp procedures on real-world objects from the YCB object set [19]. The 3-D object models, object masses and dimensions are available at [19]. A non-physical simulation environment was constructed in the RoboDK robotic simulator. The simulation environment mimics the real-world environment to an extent, containing the robotic arm, the variable-structure hand and surrounding objects.

Following the grasp control sequence shown in Fig. 8, a full grasp procedure is as such:

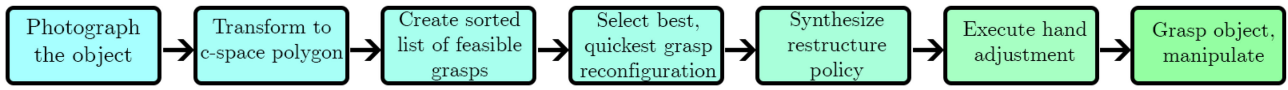


Fig. 8. A flowchart of the control sequence. These are the steps the system takes from acquisition of an object to its manipulation.

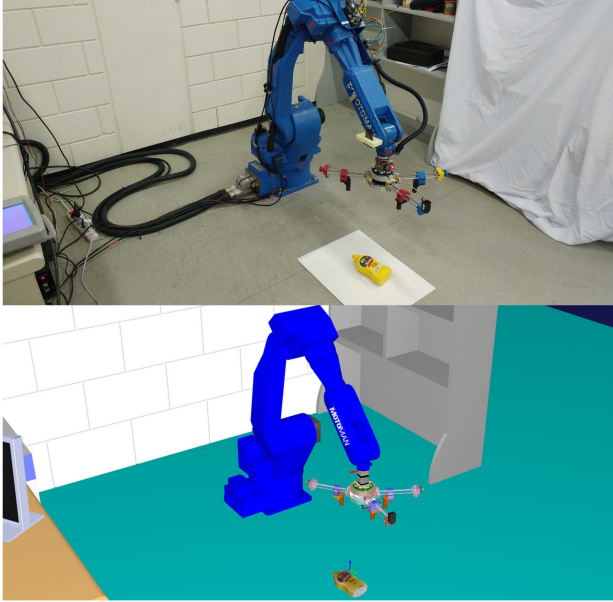


Fig. 9. The experimental setup. The real-world experiments (top) mirror the simulation environment (bottom). A “mustard bottle” item is in the pickup zone.

- 1) The robot hand is set at an arbitrary structure, usually the last structure used.
- 2) An item is placed within the pickup zone on the ground near the robot.
- 3) The robot photographs the object, and attains its shape as a polygon.
- 4) The grasp configuration and hand adjustment procedure are found, using the methods detailed in Section III.
- 5) The robot executes the hand adjustment procedure, using either a nearby wall, or the robotic arm base (user’s choice).
- 6) The hand moves towards the object, and grasps it without force feedback.
- 7) The object is manipulated towards a drop-off point, where it is placed.

A partial grasp procedure is the same as a full grasp procedure, but without the physical act of grasping and manipulation. Full grasp procedures were performed on the following objects in the YCB object set: mustard bottle (object 6), tuna fish can (object 7), power drill (object 35). Partial grasp procedures were performed on objects 4, 11, 12, 13, 21, 22, 29, 33, 51, 52, 76, 77. All grasp procedures were performed using the three-finger hand depicted in Fig. 9. Three different types fingertip offsets were used, that differ only in their minimal and maximal distances from the hand center. Fingertip offsets were selected based on object size.

A. Representing the Object as a Polygon

In order to apply the grasp selection method described in Section III, we first convert the previously unknown object to a polygon. To do this, the robot arm takes an image of the object using an arm-mounted webcam. The image is contrast balanced and converted to black and white. Noise is removed via a “close” morphology operator, along with several other standard image processing operations to clean the image. The object is now represented as a single “blob”. The object is converted to a configuration space object by using an “erode” morphology operator, whose kernel is a disc with the radius of the fingertips. The blob’s perimeter is then taken as a list of pixel locations. Since this list is finite, the blob is inherently represented as a polygon. This polygon is simplified (the number of edges is reduced), according to a tolerance set by the user. A lower tolerance results in a better approximation to the original blob and a higher number of edges. However, it may result in undesirable sharp corners that misrepresent the object’s surface normal. A higher tolerance results in a worse approximation of the blob, and a lower number of edges. The remainder of our algorithm is indifferent to the number of polygon edges, therefore the tolerance is set by trial and error, avoiding oversimplification on one hand, and artificial sharp corners on the other. The final polygon is then passed to the next portion of the procedure—grasp selection.

B. Execution of the Hand Adjustment Procedure

Following grasp selection (Section III) and adjustment procedure synthesis (Section IV), a list of instructions is provided. When followed, this list of instructions transforms the hand from its initial structure to its target structure suited to grasp the object. An Arduino Nano controls the stepper motor in the robot hand. Rotation validation is obtained by a rotary encoder fixed to the thumb. The instructions can be carried out in simulation mode, or in *run-on-robot* mode. For safety reasons, experiments were carried out in simulation mode, before being replicated in run-on-robot mode. Implementation of the full grasp procedure can be seen in the video clip accompanying this paper.

C. Experiment Results

Three objects were grasped and manipulated using the full grasp procedure, while twelve additional objects were used for partial grasp procedures. In all fifteen cases, the system was able to find grasp configurations, synthesize the adjustment procedure, and realize the change in hand structure. Objects 11, 12 and 77 are relatively small, therefore fingertips with a small minimal distance were used. Similarly, fingertips with a large maximal distance were used for the larger object 33.

The other objects were grasped using mid-range fingertips. The mean structure re-adjustment time was 63 seconds ($\sigma = 22$ s), although it should be noted that both the robotic arm and hand were operated at slow speeds for safety. Limited tests have shown a *ten-fold improvement* in the hand re-adjustment time when the safety features are disabled.

In the full manipulation tasks, both the can and bottle were manipulated successfully. The power drill was grasped, but slipped from the hand during manipulation. This slippage was due to low grasp forces by design, as part of the experimental safety measures. The force exerted by each fingertip was at most $F = 5$ N. Furthermore, the fingertips used had a low friction coefficient of $\mu = 0.4$ with the objects, reducing grasp robustness. A simple quasi-static grasp criterion gives the maximum weight that can be lifted by k fingertips without slippage $m_{max} \cdot g = kF\mu$. In the case of the power drill picked up by a 3-fingered hand, $m_{max} \cdot 9.8 = 3 \cdot 5 \cdot 0.4$, allowing a maximum mass of $m_{max} = 0.2$ kg which is *lower* than the power drill's actual mass of 0.9 kg, leading to the failed manipulation. The next step in our experiments would be to relax the safety restrictions, thus increasing the grasp force and drastically reducing the hand readjustment time.

VI. CONCLUSION

The paper introduced a novel variable-structure robotic hand that uses the environment to adjust its structure prior to grasping an object. A design example of such a hand, as well as basic algorithms needed to choose the grasp and adjust the hand structure using the environment were discussed. Initial experiments show how the robotic hand can be used as part of a full system, from image capture of an object, through hand structure synthesis, to full object manipulation.

The work reported in this paper is currently being extended to increase adjustment speed by relaxing safety restrictions. Short term continuation of this work also includes the development of tools that will determine the optimal number of digits to use for a given set of objects. Future work will also investigate the option to press or release multiple finger plungers simultaneously. This may allow shorter hand adjustment times through design. Another issue concerns the hand's size. Since the hand is relatively large, it is not suited to work in confined spaces. Also, we intend to explore the combination of more complex fingertips, readily available with integrated technology, such as [11] or [12].

As for long term goals, the variable-structure hand opens an entire new horizon of incorporating the environment in manipulation. Not only in basic grasps, but in subsequent manipulations tasks. Beyond the current research, we plan to show that variable-structure hands can have a much wider range of applications when performing complex manipulation tasks. To do that, our greatest challenge would be the design of variable-structure 3-D hands. We know that three fingers and a palm, or alternatively four fingers, can secure arbitrary 3-D objects, even under low-friction conditions. Can such hands adjust their structure using the environment, while closing with a single

actuator like industrial grippers? We are particularly looking into the creation and adjustment of virtual temporary joints [20] using the environment as a temporary joint to adjust the hand structure in 3-D domains.

ACKNOWLEDGMENT

The authors would like to thank Yarden Zohar and Liav Abrams for their contributions in the Monte-Carlo simulation and the image processing parts of the experiments.

REFERENCES

- [1] A. Bicchi, "Hands for dexterous manipulation and robust grasping: A difficult road toward simplicity," *IEEE Trans. Robot. Autom.*, vol. 16, no. 6, pp. 652–662, Dec. 2000.
- [2] J. Mahler *et al.*, "Learning ambidextrous robot grasping policies," *Sci. Robot.*, vol. 4, no. 26, 2019, Paper eaa4984.
- [3] S. B. Backus and A. M. Dollar, "An adaptive three-fingered prismatic gripper with passive rotational joints," *IEEE Robot. Autom. Lett.*, vol. 1, no. 2, pp. 668–675, Jul. 2016.
- [4] A. M. Dollar and R. D. Howe, "A robust compliant grasper via shape deposition manufacturing," *IEEE/ASME Trans. Mechatronics*, vol. 11, no. 2, pp. 154–161, Apr. 2006.
- [5] J. Shintake, V. Cacucciolo, D. Floreano, and H. Shea, "Soft robotic grippers," *Adv. Mater.*, vol. 30, no. 29, 2018, Art. no. 1707035.
- [6] S. Terryn, J. Brancart, D. Lefeber, G. Van Assche, and B. Vanderborght, "Self-healing soft pneumatic robots," *Sci. Robot.*, vol. 2, no. 9, pp. 1–12, 2017.
- [7] F. Ilievski, A. D. Mazzeo, R. F. Shepherd, X. Chen, and G. M. Whitesides, "Soft robotics for chemists," *Angewandte Chemie Int. Ed.*, vol. 50, no. 8, pp. 1890–1895, 2011.
- [8] E. Brown *et al.*, "Universal robotic gripper based on the jamming of granular material," *Proc. Nat. Acad. Sci.*, vol. 107, no. 44, pp. 18 809–18 814, 2010.
- [9] R. Deimel and O. Brock, "A novel type of compliant and underactuated robotic hand for dexterous grasping," *Int. J. Robot. Res.*, vol. 35, no. 1-3, pp. 161–185, 2016.
- [10] Y. Golan, A. Shapiro, and E. Rimon, "Synthesis of an adjustment procedure for a variable configuration robotic hand," Robotics Lab, Ben-Gurion University, Israel, Be'er Sheva, Israel, Tech. Rep., 2020. [Online]. Available: <http://robotics.bgu.ac.il/mw/images/9/97/vhr.pdf>
- [11] Y. Yang, Y. Chen, Y. Li, Z. Wang, and Y. Li, "Novel variable-stiffness robotic fingers with built-in position feedback," *Soft Robot.*, vol. 4, no. 4, pp. 338–352, 2017.
- [12] Y. Golan, A. Shapiro, and E. Rimon, "Jamming-free immobilizing grasps using dual-friction robotic fingertips," *IEEE Robot. Autom. Lett.*, vol. 5, no. 2, pp. 2889–2896, Apr. 2020.
- [13] E. Rimon and J. W. Burdick, "New bounds on the number of frictionless fingers required to immobilize planar objects," *J. Robot. Syst.*, vol. 12, no. 6, pp. 433–451, 1995.
- [14] SMC Inc. Slide guide round body air Gripper 3-finger type MHS3, 2020. [Online]. Available: <https://www.smcin.com/content/slide-guide-round-body-air-gripper-3-finger-type-mhs3>
- [15] E. Rimon and J. Burdick, *The Mechanics of Robot Grasping*. Cambridge, U.K.: Cambridge Univ. Press, 2019.
- [16] H. A. Bunis, E. D. Rimon, Y. Golan, and A. Shapiro, "Caging polygonal objects using formationally similar three-finger hands," *IEEE Robot. Autom. Lett.*, vol. 3, no. 4, pp. 3271–3278, Oct. 2018.
- [17] E. Rimon and A. Blake, "Caging planar bodies by one-parameter two-fingered gripping systems," *Int. J. Robot. Res.*, vol. 18, no. 3, pp. 299–318, 1999.
- [18] Y. Golan. Variable configuration hand GitHub repository, 2020. [Online]. Available: <https://github.com/Yoavgolani/Variable-Configuration-Hand-Operation>
- [19] B. Calli, A. Walsman, A. Singh, S. Srinivasa, P. Abbeel, and A. M. Dollar, "Benchmarking in manipulation research: Using the Yale-CMU-Berkeley object and model set," *IEEE Robot. Autom. Mag.*, vol. 22, no. 3, pp. 36–52, Sep. 2015.
- [20] A. Sintov and A. Shapiro, "Swing-up regrasping algorithm using energy control," in *Proc. IEEE Int. Conf. Robot. Autom.*, 2016, pp. 4888–4893.